Journal of Applied Electrochemistry **33**: 1063–1068, 2003.

Hydrophobic interfacing layers for improvement of corrosion protection by polymeric coatings

S-Y. ZHANG*, Y. KONG, Z-S. ZHANG and X-Y. ZHANG
School of Chemistry and Chemical Engineering, Shandong University, Jinan, 250100 P.R. China
*(*author for correspondence, e-mail: syzhang@sdu.edu.cn)*

Received 23 October 2002; accepted in revised form 9 May 2003

Key words: corrosion protection, interfacial layer, polymeric coating, self-assembled monolayer

Abstract

Water sorption of coating materials is the main cause of coating deterioration, adhesion loss and substrate corrosion. By introducing alkanethiol self-assembled monolayers (SAMs), a hydrophobic interfacing layer between coating and substrate metal can be constructed. The effect of the hydrophobic SAMs interfacing layer on the corrosion protection of epoxy coatings was evaluated using electrochemical techniques including Tafel polarization, electrochemical impedance spectroscopy and impedance–time transition measurement. It was found that the SAMs interfacing layer improved the corrosion protection of the coating significantly. The improvement was attributed to the strong interaction between SAMs and the metal substrate, the compact structure and low water affinity of the SAMs interfacing layer, which prevent water absorbed by the coating from reaching the coating–metal interface and spreading along the interface.

1. Introduction

To coat metals with polymeric coatings which form protective barrier layers on the metal surface is the most convenient and most effective way of protecting metals from corrosion. It is obvious that coatings with defects such as cracks, pinholes and bubbles cannot provide good protection. However, owing to water sorption of coating materials, even defect-free coatings cannot offer perfect and permanent protection.

Polymers used as coating materials are all polar. For example, cured epoxy resins contain a large number of polar groups such as hydroxyl groups, amino groups and epoxy groups. By forming hydrogen bonds or even chemical bonds with the substrates, these polar groups can help to improve coating adhesion [1]. Unfortunately, water sorption of the coatings also increases due to the high content of polar groups [2, 3]. Water absorbed by coatings not only swells the coatings and lowers the glass transition temperature of the coatings [3–7], but also creates voids and cracks in the coating matrix due to structural tension generated during swelling [3, 8–10]. In addition, with defects or intermolecular voids serving as passages, water can diffuse through the coating. On reaching the substrate surface, water will initiate or accelerate corrosion of the substrate metal, weakening or even destroying the adhesion between coating and metal [1–3, 11–15]. Therefore, to improve corrosion protection by polymeric coatings, water sorption of the coating materials must be reduced and the diffusion of water to the coating–metal interface must be slowed down.

As demonstrated in the literature, free volume and water affinity are the two main factors in determining water sorption of resins [2, 3, 16–18]. Therefore, water sorption of the resin can be lowered either by minimizing free volume in the resins or by reducing water affinity of the resins. By optimizing the curing procedure [3, 18, 19] or using curing accelerators with appropriate catalytic activity [20], coatings with more compact structure and, therefore, less free volume can be obtained. For cured resins, free volume can be reduced usually by physical annihilation of the resins [21, 22].

Non-polar polymers with free volume do not absorb water, which suggests that free volume with no neighboring hydrophilic groups is inaccessible to water [2–4]. However, it is impossible to remove polar groups from the resins. The water affinity of the resins can be reduced either by substitution of the polar groups for less hydrophilic ones or by introduction of fluorine atoms into the polymers. For example, when epoxy resins are cured with active esters, only ester groups, which are much less hydrophilic than hydroxyl groups, are present in the resultant resin [23–27]. Water sorption of the ester-cured resins is only about 50% of that of common resins and the corrosion protection of the coating can be markedly improved [27–30].

When fluorinated polymers are used instead of conventional polymers, water sorption of the cured resins can also be reduced significantly [31, 32]. How-

ever, because of their high prices, it is impossible for fluorinated polymers to become common coating materials in the near future.

Besides reducing water sorption of the coating, reduction of free volume and lowering of water affinity also narrows water passages in the coating and slows down the transport of water through the coating [28–30]. Water passages in polymeric coatings can also be interrupted by introduction of flake-shaped additives, such as mica. Such additives can retard or block the transport of water in the coating and physically improve the corrosion protection of the coating.

In the present work, we introduce a third way of improving corrosion protection of epoxy coatings by insertion of a hydrophobic alkanethiol self-assembled monolayer (SAM) between the coating and the metal substrate.

2. Experimental details

2.1. *Materials*

n-dodecanethiol (DT) of AR grade from Shreagent Co. Ltd, Shanghai, China, was used as received. For preparation of DT self-assembled monolayer (DT SAMs), a dilute alcohol solution with 10^{-3} mol dm^{-3} DT was prepared by dissolving DT in AR absolute alcohol.

Epoxy coatings used for the present study were prepared by curing YDCN-702p *o*-cresol novolac epoxy resin (ECN), from Tohto Kasei, Japan, with H-1 phenol novolac resin (NOV) from Sumitonmo, Japan. 2-methylimidazole (2MI) from Wuhan Pharmaceutical Co., China, was used as curing accelerator. The fresh mixture of ECN, NOV and 2MI in a weight ratio of 1:0.5:0.0075 was dissolved in 12 ml of AR acetone before use.

2.2. *Preparation of SAMs and epoxy coatings*

A copper electrode with an exposed area of 1.0 cm^2 was made by mounting a copper disc in an epoxy electrode holder. The electrode was polished with emery paper until the surface of the copper attained a mirror-like finish. After polishing, the electrode was wiped three times with AR alcohol and then rinsed with deionized water for 30 s.

DT SAMs on copper was prepared by dipping the electrode in an alcohol solution of DT for 30 min.

To ascertain whether or not the immersion of SAMs in AR acetone (the solvent for preparation of the epoxy coating) had significant detrimental effect on the structure of the DT SAMs, a SAMs-coated electrode was treated by immersion in acetone for 30 s and then subjected to electrochemical tests.

Epoxy coatings about 10 μm thick were prepared by dipping the naked copper electrode and the SAMs-coated electrode in an acetone solution containing ECN, NOV and 2MI for 30 s. The electrodes were left in the open air for 1 day and then cured in a vacuum furnace according to the procedure reported elsewhere [24]. In this way, both the epoxy-coated electrode and the electrode with a SAMs interfacing layer were prepared.

2.3. *Electrochemical measurements*

For electrochemical measurements, a conventional three-electrode cell was used. Four kinds of electrodes (i.e., the naked copper electrode, SAMs-coated electrode, epoxy-coated electrode and SAMs interfacing epoxy-coated electrode) were used as working electrodes. A 0.5 mol dm^{-3} NaCl solution prepared with AR NaCl and deionized water was the electrolyte. A platinum coil electrode and a saturated calomel electrode (SCE) were used as auxiliary electrode and reference electrode, respectively. All potentials reported in this paper refer to the SCE reference electrode.

All electrochemical measurements were conducted using a CHI 604A electrochemical analyser (CH instrument, USA). Tafel polarization was performed within the range −0.4 to −0.05 V with a scan rate of 10 mV s^{-1}. For evaluating the corrosion behaviour of copper under different protective coatings, electrochemical impedance spectroscopy (EIS) and impedance–time measurement were applied. The impedance spectra were recorded at open circuit potential after 30 min of immersion in the NaCl solution between 1×10^5 and 2×10^{-2} Hz with alternating current amplitude of 5 mV.

Analysis of the impedance spectra was performed using EG&G PARC EQUICRT impedance modelling software using the equivalent circuits shown in Figure 1. For simplicity, only the spectrum frequency ranging between 10^5 and 10^2 Hz, which corresponds to the semicircle in the impedance spectrum at high frequency, was selected for analysis.

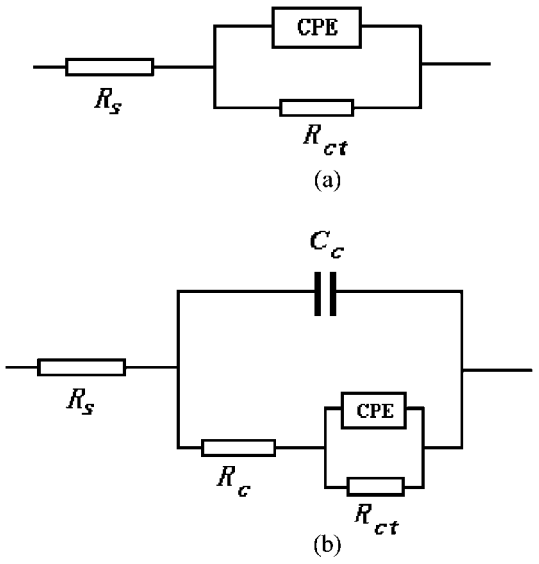

Fig. 1. Equivalent circuits for the naked copper electrode (a) and SAMs-coated electrode, epoxy-coated electrode and SAMs interfacing epoxy-coated electrode (b) R_s, solution resistance; R_c, coating resistance; C_c, coating capacitance, CPE, constant phase element for the coating–metal interface; R_{ct}, interfacial charge transfer resistance.

The impedance–time transition measurement was also conducted at open circuit potential at 962 Hz for 10 h.

3. Results and discussion

3.1. *Effect of solvent immersion*

For evaluation the effect of acetone immersion on the structure of the DT SAMs, the SAMs-coated electrode and the acetone-immersed electrode was elucidated by electrochemical polarization, respectively. The Tafel plots obtained for the two electrodes are shown in Figure 2.

It can be seen that, after immersion in acetone, the corrosion potential of the SAMs-coated electrode shifts slightly to the positive and the corrosion current also decreases slightly. However, the difference in the Tafel plots between these two electrodes is so small that it is reasonable to neglect the effect of acetone immersion on the structure of SAMs. This showed that, owing to the strong chemical interaction between DT and the copper surface, the DT SAMs can withstand solvent immersion during the application of epoxy coatings. Small changes in the structure of the SAMs after preparation of the epoxy coating are also apparent from the results obtained from electrochemical impedance spectroscopy and impedance–time transition measurement for the SAMs interfacing electrode (*vide infra*).

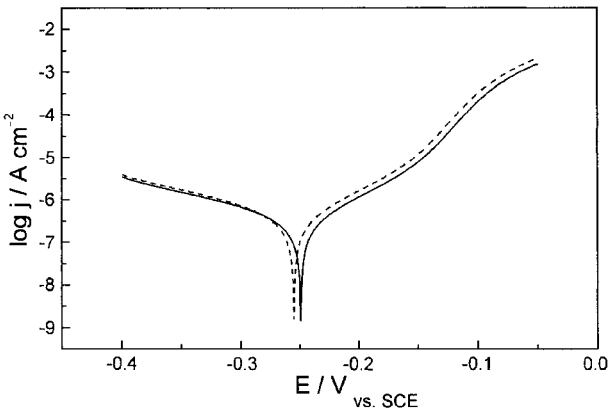

Fig. 2. Tafel plots for the SAMs-coated electrode and acetone-immersed SAMs-coated electrode. Potentials are referenced to the SCE. Key: (- - -) SAMs-coated electrode, (—) acetone-immersed electrode.

The positive shift in corrosion potential and the slight decrease in corrosion current even suggest a small improvement in the assembly of DT during acetone immersion. Known as the solvent effect, this phenomenon has also been observed by other researchers [38].

3.2. *Electrochemical impedance measurement*

Figure 3 presents the fitted Nyquist plots for the four electrodes.

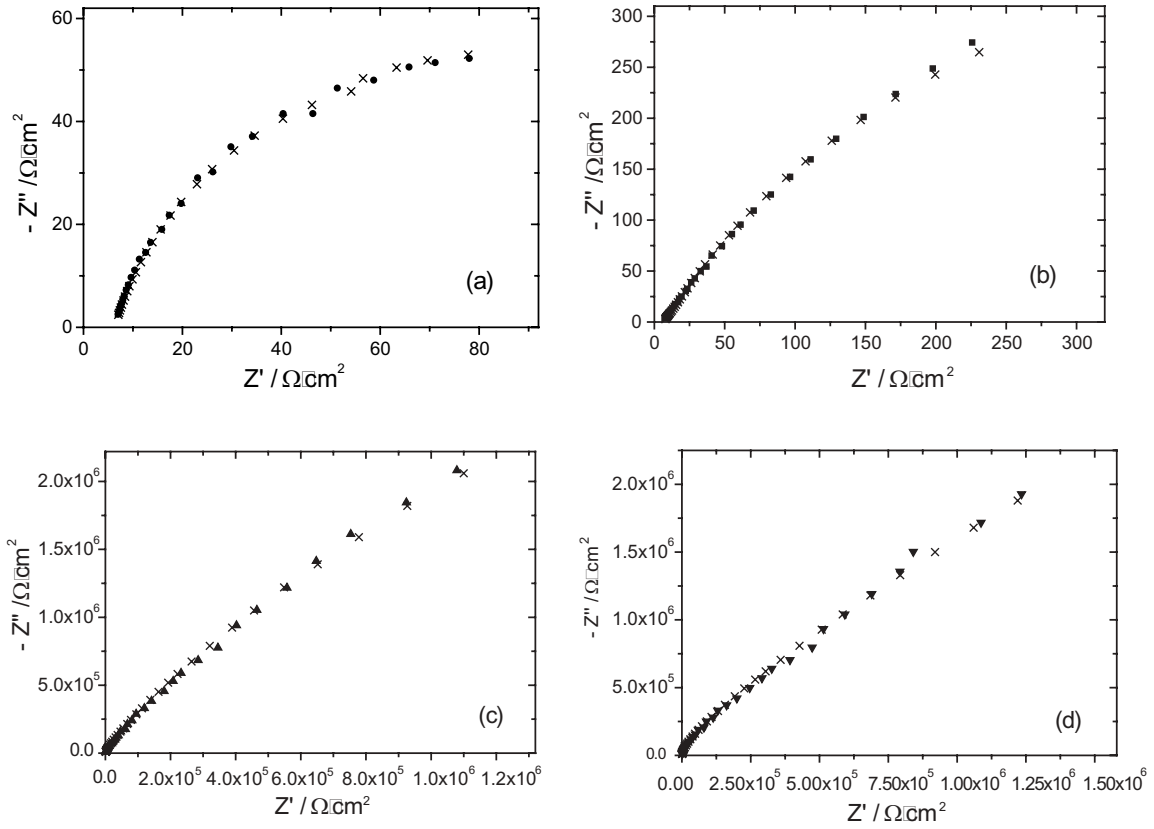

Fig. 3. The fitted Nyquist Plots for the four kinds of electrodes in 0.5 mol dm^{-3} NaCl solution. Key: (a) naked electrode, (b) SAMs-coated electrode, (c) epoxy-coated electrode, and (d) SAMs-interfacing epoxy-coated electrode.

Table 1. Coating resistance (R_c) and interfacial charge-transfer resistance (R_{ct}) of the four electrodes

Electrodes	Naked copper	SAMs-coated electrode	Epoxy-coated electrode	SAMs-interfacing epoxy coated electrode
$R_c/\Omega\ cm^2$		15	1.5×10^5	1.8×10^5
$R_{ct}/\Omega\ cm^2$	1.4×10^2	1.1×10^3	4.5×10^6	7.1×10^7

In our study, only the coating resistance (R_c) and interfacial charge transfer resistance (R_{ct}) were concerned. Only the data in the high frequency region, in which the electrode reaction is controlled mainly by charge transfer resistance R_{ct}, were analysed, excluding the low frequency region which is related mainly to the Warburg impedance corresponding to semi-infinite linear diffusion. Therefore, the equivalent circuits used, shown in Figure 1, are much simpler than those usually used for interpretation of whole impedance spectra [37]. As shown in Figure 3, the fitting data coincides well with the experimental results and the chi-squares of the fit are all of the magnitude of 10^{-4}.

The coating resistance and coating–metal interfacial charge transfer resistance obtained through NLLS fitting are listed in Table 1.

It can be seen that R_{ct} of the SAMs-coated electrode, $1.1 \times 10^3\ \Omega$, was about 10 times larger than that of the naked copper electrode, $1.4 \times 10^2\ \Omega$. This reveals the inhibition effect of the DT SAMs [35–37]. The coverage of DT SAMs (θ) can be calculated according to the following equation

$$(1 - \theta) = \frac{R_{ct}^0}{R_{ct}} \quad (1)$$

where R_{ct}^0 and R_{ct} are the values for the naked copper electrode and the SAMS-coated electrode, respectively. The coverage of DT SAMs for our electrode was calculated to be 87.3%, which suggests that there were unfilled defects in our DT monolayer.

As shown in Table 1, R_c of the epoxy-coated electrode and the SAMs interfacing epoxy-coated electrode were nearly the same. Thus, the thickness of these two coatings was similar. The R_c of the epoxy coating was more than 10^5 times larger than that of the DT SAMs alone, which can be attributed to the greater thickness and perfect structure of the coating. That is, the epoxy coating of about 10 μm was $10^3 \sim 10^4$ times thicker than that of the DT monolayer of only several angstroms and the coverage of the epoxy coating was much better than that of the DT monolayer.

The R_{ct} of the epoxy-coated electrode and the SAMs interfacing epoxy-coated electrode were both $10^3 \sim 10^4$ times higher than that of the SAMs-coated electrode. The high R_{ct} indicates better corrosion protection by the epoxy coating. The R_{ct} of the SAMs interface epoxy-coated electrode was about 20 times larger than that of the epoxy-coated electrode, so the introduction of SAMs could indeed improve the corrosion protection of the epoxy coating.

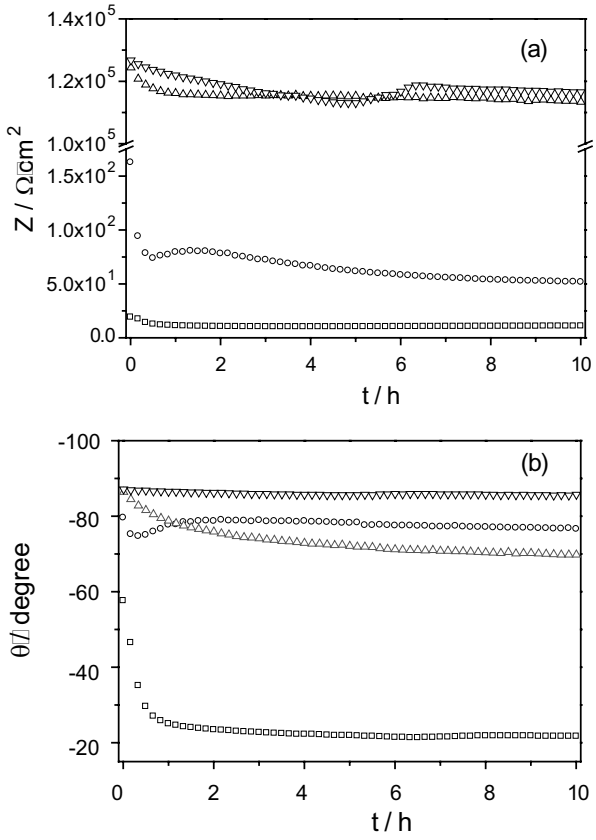

Fig. 4. Impedance–immersion time transition (a) and phase angleimmersion time transition (b) plots for the four electrodes in 0.5 mol dm^{-3} NaCl solution. Key: (□) naked electrode, (○) SAMs-coated electrode, (△) epoxy-coated electrode, and (▽) SAMs interface epoxy-coated electrode.

3.3. *Impedance–time transition measurement*

The impedance transition of the naked copper electrode and copper under protection of various barrier layers as a function of immersion time in NaCl solution were monitored using an electrochemical-time technique. The impedance–time transition and the phase angle–time transition thus obtained are shown in Figure 4.

In Figure 4(a), the impedance of the SAMs coated-electrode dropped significantly at the early stage of immersion. A slight impedance recovery occurred at about 30 min. The impedance drop can be attributed to penetration of the NaCl solution towards the copper surface through the unfilled defects in the SAMs [35–37]. The slight impedance recovery may be due to migration of coordinated clusters to the unfilled defects in the SAMs [38].

The impedance of the epoxy-coated electrode and the SAMs interfacing electrode shown in Figure 4(a) were much higher than that of the SAMs-coated electrode as demonstrated by the impedance measurements (cf. Figure 3).

It is well known that the phase angle is more sensitive to the state change of both coating and metal surface than impedance [11, 39, 40]. The phase angle transitions of the four systems depicted in Figure 4(b) show that the phase angle of the naked copper electrode shifted significantly to the positive from −58.9° to −21.7° during the 10 h immersion. The positive shift of the phase angle suggests rapid corrosion of copper in 0.5 mol dm^{-3} NaCl solution. According to Figure 4(a), the impedance of the SAMs-coated electrode dropped sharply at the early stage of immersion, but the phase angle of this electrode remained nearly unchanged during the whole immersion period as shown in Figure 4(b). The drop in impedance may be attributed partially to corrosion of the substrate and partially to damage to the SAMs barrier layer. However, as seen in Figure 4(b), both the corrosion of the substrate and the damage to the SAMs barrier layer were not serious. This means that although the impedance of the SAMs layer was low, its corrosion protection was significant [35–37].

Figure 4(b) also demonstrates that the initial phase angles for both the epoxy-coated electrode and the SAMs interfacing epoxy-coated electrode were much more negative than that of the SAMs-coated electrode, which suggests a better barrier effect for the epoxy coatings. It is also interesting that, although the impedance of the epoxy-coated electrode was nearly the same as that of the SAMs interfacing epoxy-coated electrode (cf. Figure 4(a)), the phase angle transition behaved rather differently. The phase angle of the epoxy-coated electrode shifted from −86.4° to −69.7° while that of the SAMs-interfacing epoxy coated electrode only changed from −87.1° to −85.6°. This suggests that the state change of the epoxy-coated electrode was much more significant than that of the SAMs interfacing epoxy-coated electrode.

As mentioned above, structural changes of the coating due to water sorption and surface state changes of the substrate due to corrosion are the two main reasons for phase angle changes. Because the epoxy coatings in both epoxy-coated electrodes and SAMs interfacing epoxy-coated electrodes are the same, we hypothesized that the structural changes of the coatings due to water sorption for these two systems would be similar and the structural effects of the epoxy coatings on the phase angles for these two systems should also be similar. Therefore, the great difference in phase angle transition between these two systems can only be attributed to the difference in surface state of the substrate, that is, substrate corrosion.

According to the adhesion formation mechanism, during construction of adhesion between the coating polymer and the substrate metal, polar groups on the polymer chains usually arrange themselves towards the coating–metal interface to form as many bonds as possible with surface groups on the substrate [1, 29]. This spontaneous orientation of polar groups results in an accumulation of polar groups in the interfacial region. Since it contains more polar groups, the polymer–metal interfacial region may be more hydrophilic than the bulk coating. The hydrophilicity of the coating–metal interface promotes not only the transport of water towards the surface of the substrate metal (vertical diffusion) but also the spreading of water along the metal surface, (horizontal diffusion) as shown in Figure 5.

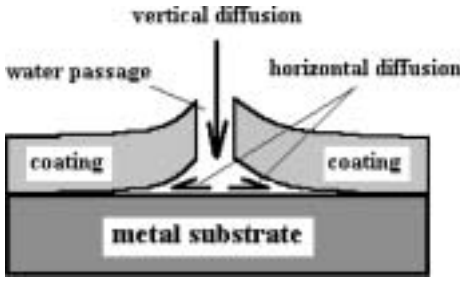

Fig. 5. Vertical diffusion of water through water passages in the coating and horizontal diffusion of water along the coating–metal interface.

The horizontal diffusion of water is the main source of substrate metal surface wetting. The progress of both corrosion of the substrate and delamination of the coating is the direct result of the advancing wetted area. Therefore, for a polymer-coated metal system with a more hydrophilic coating–metal interface, rapid corrosion of the substrate metal may occur even though the appearance of the coating remains perfect and the resistance of the coating stays high [11, 39, 40].

It is interesting that the change in phase angle for the SAMs monolayer with low resistance was not as significant as that of the epoxy-coated electrode with high resistance. As pointed out above, the epoxy–metal interface may be more hydrophilic than the bulk coating due to accumulation of polar groups. However, for DT–metal interface, the case is rather different. First, the mercapto groups (–SH) in alkanethiols can form such strong interactions with copper that it is difficult to replace the DT–metal interface with a water–metal interface. Such replacement is a major cause of adhesion loss and coating delamination for epoxy coatings [1]. Second, owing to both the low water affinity and the compact assembly of mercapto groups, the water affinity of the DT–metal interface is low and the free volume in the DT–metal interfacial region is small. Both of these factors make it difficult for water molecules to diffuse horizontally through the DT assembly. We thus attribute the phase angle transition characteristics of the SAMs-coated electrode and the SAMs interfacing epoxy-coated electrode to (i) the strong interaction between DT and metal substrate; (ii) the low water affinity of the DT monolayer; and (iii) the compact structure of the DT–metal interface.

The interfacial SAMs layer is somewhat like that formed in the epoxy-coated metal system prepared by curing *o*-cresol novolac epoxy resin with phenol novolac acetate resin as hardener [29, 30]. In fact, adsorption of either a physical or a chemical nature is a consequence

for any interface system. Our previous results and the above discussion all suggest that during application of polymers to metal, the coating polymers, the organic additives and the inorganic particles are all possibly adsorbed onto the substrate surface. Although it is virtually impossible for coating polymers, organic additives and inorganic particles to form perfect monolayers like alkanethiols on Au and Cu, even a partial adsorption layer may affect both adhesion and corrosion protection of the coating. It is apparent that adsorption at the coating–metal interface deserves further investigation for comprehensive understanding of the corrosion protection mechanisms of polymeric coatings.

4. Conclusions

(i) The effect of post preparation of polymeric coatings on the structure of the alkanethiol SAMs on copper is small.
(ii) By introducing alkanethiol SAMs between the coating and the substrate, an interfacial layer with strong interaction with the substrate and high interfacial hydrophobicity can be constructed. This interfacial SAMs layer improves the corrosion protection of the polymeric coating significantly.

Acknowledgement

We thank Nature Science Foundation of China for financial support and Miss P. Holt for English improvement.

References

1. R.G. Schmidt and J.P. Bell, *in* K. Dusek (Ed.), 'Advance in Polymer Science', Epoxy Resins and Composites II (Springer-Verlag, New York, 1986), pp. 33–71.
2. S-Y. Zhang, X-W. Luo, S-J. Li and W-F. Zhou, *Huaxue Tongbao* **8** (1997) 31.
3. M.C. Lee and N.A. Peppas, *Prog. Polym. Sci.* **18** (1993) 947.
4. P. Moy and F.E. Karasz, *Polym. Eng. Sci.* **20** (1980) 315.
5. P. Nogueira, C. Ramirez, A. Torres, M.J. Abad, J. Cano, J. Lopez, I. Lopez-Bueno and L. Barral, *J. Appl. Polym. Sci.* **80** (2001) 71.
6. E.P.M. van Westing, G.M. Ferrari and J.H.W. De Wit, *Electrochim. Acta* **39** (1994) 899.
7. E.P.M. van Westing, G.M. Ferrari and J.H.W. De Wit, *Corros. Sci.* **36** (1994) 957.
8. D.J. Belton, E.A. Sullivan and M.J. Molter, *in* J.H. Lupinski and R.S. Moore (Eds.), 'Polymeric Materials for Electronics Packaging and Interconnection', ACS symposium Series 407 (American Chemical Society, Washington, DC, 1989), p. 286–320.
9. Z.R. Xu and K.H.G. Ashbee, *J. Compos. Mater.* **25** (1991) 760.
10. T.C. Wong and L.J. Broutman, *Polym. Eng. Sci.* **25** (1985) 529.
11. F. Mansfeld, *J. Appl. Electrochem.* **25** (1995)187.
12. F. Mansfeld, L.T. Han, C.C. Lee and G. Zhang, *Electrochim. Acta* **43** (1998) 2933.
13. R.D. Armstrong, J.D. Wright and T.M. Handyside, *J. Appl. Electrochem.* **22** (1992) 795.
14. R.D. Armstrong and J.D. Wright, *Electrochim. Acta* **38** (1993) 1799.
15. Y-H. Chen, S-J. Li, C. Pu and W-F. Zhou, *Acta Chimica Sinica* **53** (1995) 328.
16. V.B. Gupta, L.T. Drzal and M.J. Rich, *J. Appl. Polym. Sci.* **30** (1985) 4467.
17. T. Suzuki, Y. Oki, M. Numajiri, T. Miura, K. Konda, Y. Shimoni and Y. Ito, *Polymer* **37** (1996) 3025.
18. M.T. Aronhime, X. Peng, J.K. Gillham and R.D. Small, *J. Appl. Polym. Sci.* **32** (1986) 3589.
19. J.B. Enns and J.K. Gillhan, *J. Appl. Polym. Sci.* **28** (1983) 2831.
20. X-W. Luo, Z-Y. Yun, S-J. Li and W-F. Zhou, *Macromol. Rapid Commun.* **16** (1995) 941.
21. S-Y. Zhang, PhD thesis, Fudan University, Shanghai (1998).
22. P.H. Pfromm and W.J. Koros, *Polymer* **36** (1995) 2379.
23. X-W. Luo, Z-H. Ping, J-P. Ding, Y-D. Ding and S-J. Li, *J. Macromol. Sci. A* **34** (1997) 2279.
24. S-J. Li, S-Y. Zhang, X-W. Luo, Y-F. Ding and W-F. Zhou, *Chem. J. Chinese Univs.* **21** (2000) 813.
25. S. Nakamura, Y. Saegusa, H. Yanagisawa, M. Touse, T. Shirai and T. Nishikubo, *Thermochim. Acta* **183** (1991) 269.
26. S. Nakamura and M. Arima, *J. Thermal Analy.* **40** (1993) 613.
27. M. Arina, H. Ibe and S. Nakamura, *Report on Progress in Polym. Phys. Jpn.* **36** (1993) 267.
28. S-Y. Zhang, X-W. Luo, S-J. Li and W-F. Zhou, *Acta Chimica Sinica* **57** (1999) 329.
29. S-Y. Zhang, X-W. Luo, S-J. Li and W-F. Zhou, *Corros. Sci.* **42** (2000) 2037.
30. S-Y. Zhang, Y-F. Ding, S-J. Li, X-W. Luo and W-F. Zhou, *Corros. Sci.* **44** (2002) 861.
31. M. Vecellio, *Prog. Organic Coat.* **40** (2000) 225.
32. F. Deflorian, L. Fedrizzi, D. Lenti and P.L. Bonora, *Prog. Organic Coat.* **22** (1993) 39.
33. F. Deflorian, L. Fedrizzi and P.L. Bonora, *Prog. Organic Coat.* **23** (1993) 73.
34. V.E. Miskovic-Stankovic, F. Deflorian, P.L. Bonora and L. Fedrizzi, *Prog. Organic Coat.* **24** (1994) 253.
35. Y. Feng, W-K. Teo, K-S. Siow, Z. Gao, K-L. Tan and A-K. Hsieh, *J. Electrochem. Soc.* **144** (1997) 55.
36. D. Taneichi, R. Haneda and K. Aramaki, *Corros. Sci.* **43** (2001) 1589.
37. Z-L. Quan, S-H. Chen and S-L. Li, *Corros. Sci.* **43** (2001) 1071.
38. A. Ulman, *Chem. Rev.* **96** (1996) 1533.
39. E.P.M. van Westing, G.M. Ferrari, F.M. Geenen and J.H.W. de Wit, *Prog. Organic Coat.* **23** (1993) 89.
40. E.P.M. van Westing, G.M. Ferrari and J.H. W. de Wit, *Corros. Sci.* **36** (1994) 979.